The Noise Performance of Electron Multiplying Charge-Coupled Devices

Mark Stanford Robbins, *Senior Member, IEEE,* and Benjamin James Hadwen

***Abstract*—Electron multiplying charge-coupled devices (EMCCDs) enable imaging with subelectron noise up to video frame rates and beyond, providing the multiplication gain is sufficiently high. The ultra-low noise, high resolution, high-quantum efficiency, and robustness to over exposure make these sensors ideally suited to applications traditionally served by image intensifiers. One important performance parameter of such low-light imaging systems is the noise introduced by the gain process. This work investigates the noise introduced by the electron multiplication within the EMCCD. The theory and measurements of the excess noise factor are presented. The measurement technique for determining the excess noise factor is described in detail. The results show that the noise performance matches that of the ideal staircase avalanche photodiode. A Monte Carlo method for simulating the low-light level images is demonstrated and the results compared with practical experience.**

***Index Terms*—Charge-coupled devices (CCD), image intensifiers, low-light level imaging, noise, photon counting, single photon detection.**

I. Introduction

THE ELECTRON multiplying charge-coupled devices (EMCCDs) use impact ionization to provide high gain in the charge domain [1]. This enables performance with an equivalent input noise of much less than 1 rms electron at pixel rates up to and beyond those required for TV imaging applications. These devices have been commercially available since 2001 [2] and their ultra-low noise, high resolution, high-quantum efficiency, and robustness to over exposure make them ideally suited to applications traditionally served by image intensifiers. As well as the "traditional" image intensifier applications, they are also finding their way into novel applications that require imaging performance that has been previously unobtainable. For example, they have been used for ground-based astronomy where resolutions comparable with those obtained from the Hubble Space Telescope have been observed [3].

An important performance parameter for low-light imaging systems is the noise introduced by the gain process. A noise factor F can be defined by the following [4]:

$$F^2 = \frac{\sigma_{\text{out}}^2}{M^2\sigma_{\text{in}}^2} \tag{1}$$

where M is the mean gain and σ_{in}^2 and σ_{out}^2 are the variances of the input and output signals, respectively. If the gain process adds no noise, then the noise factor will be unity. However, the stochastic multiplication process and any loss mechanisms introduce noise. For second-generation image intensifiers the noise factors tend to lie between 1.6 and 2.2. For filmed third-generation intensifiers the noise factors range between 2 and 3.5. Excess noise factors in excess of 60 have been obtained if the bias applied across the microchannel plate is lowered to reduce the gain [5].

The basic principle of charge multiplication in the EMCCD is similar to that of the staircase avalanche photodiode in which a single charge carrier type (electrons in this case) initiates ionization. This has been studied several times theoretically (for example in [6] and [7]), where it has been shown that the excess noise factor tends to $2^{1/2}$ as the gain is increased. Hynecek presented a theory and measurements of the noise factor from an experimental EMCCD in [4]. Here, the noise factor was shown to tend to unity but the result was corrected in subsequent publications, for example in [8].

The purpose of this present work was to develop a robust method for the measurement of the excess noise factor and to compare the results obtained using devices from E2V Technologies with theoretical prediction. A Monte Carlo method has also been developed that can be used to simulate the performance of the sensor. This method is described here and some of the results are presented.

II. Principle of EMCCD Operation

Jerram *et al*. [2] and Mackay *et al*. [9] outlined the operation of the EMCCDs studied here, and a CCD described by Hynecek [4] follows a similar principle. A detailed description of the EMCCDs tested is included in this section for clarity.

The ultimate sensitivity of a conventional CCD is limited by the noise introduced by the charge to voltage conversion process and by the video chain electronics. The readout noise increases with pixel rate and so those applications requiring high sensitivity traditionally read the devices out very slowly to minimize the noise. Typical readout noise figures for scientific type devices are shown in Fig. 1. Even at the lowest readout rates, noise levels are too high to detect single photon events. As the readout rate is increased to that required for TV operation, the noise levels significantly limit the sensitivity.

The EMCCD technology removes the limitation of the output amplifier and video chain noise by applying a low-noise gain process in the charge domain, prior to the charge to voltage conversion, to boost the signal above the noise floor of the amplifier. A schematic layout showing the essential features of the EMCCD architecture for a frame transfer device is shown in Fig. 2. The image, store, and readout registers are of conventional design and benefit from many years development activity

Manuscript received December 13, 2002; revised February 28, 2003. The review of this paper was arranged by Editor D. Verret.

The authors are with E2V Technologies, Chelmsford, Essex CM1 2QU U.K.

Digital Object Identifier 10.1109/TED.2003.813462

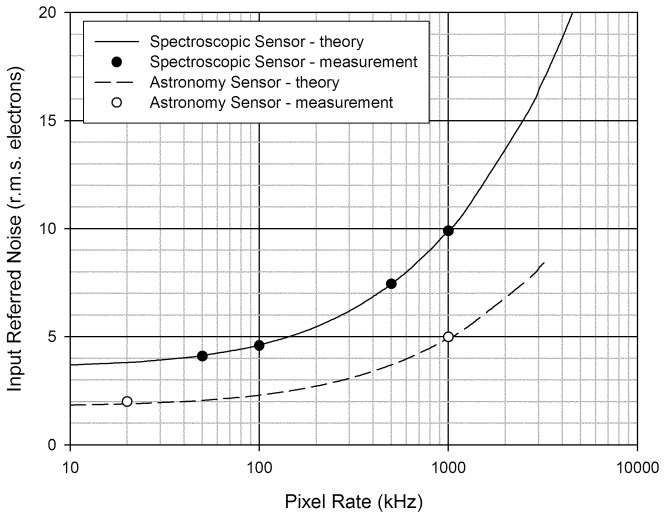

Fig. 1. Readout noise from conventional scientific type sensors. Correlated double sampling is employed with a presample filter bandwidth of twice the readout rate.

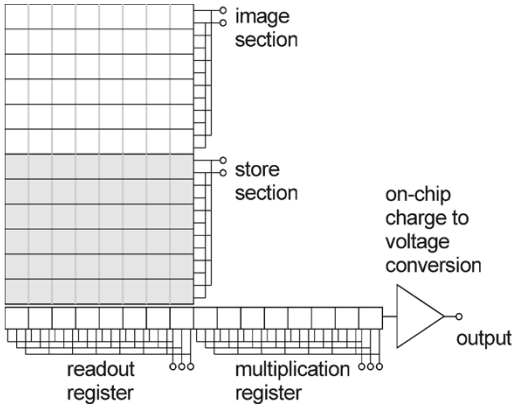

Fig. 2. Schematic of the EMCCD arrays studied here.

to optimize imaging performance. There is an additional serial register, known as the multiplication register, between the readout register and the on-chip charge to voltage conversion circuitry [10]. Each stage of the multiplication register comprises four gates, three of which are clocked. This is shown schematically in Fig. 3.

Two of the gates ($\phi 1$ and $\phi 3$) are clocked with normal amplitude drive pulses ($\sim$10 V) and can use the same pulses as those applied to two phases of the readout register. The pulses applied to $\phi 2$ of the multiplication element have higher amplitude, typically 40–45 V. A gate is placed prior to $\phi 2$, which is held at a low dc level. The potential difference between ϕdc and the high level of $\phi 2$ can be set sufficiently high so that signal electrons can undergo impact ionization processes as they are transferred from $\phi 1$ to $\phi 2$ during the normal clocking sequence. Thus, the number of electrons in the charge packet increases as it passes through a multiplication element. Although the probability of impact ionization and thus the mean gain per stage g is very low, the number of stages N can be high. The total gain of the cascaded multiplication elements is given by $M = g^N$. For 600 elements a 1.5% probability of impact ionization will give a total gain in the charge domain of over 7500.

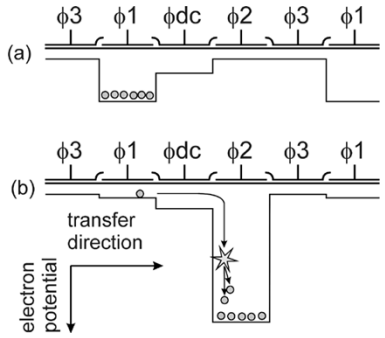

Fig. 3. Transfer of charge through a multiplication element.

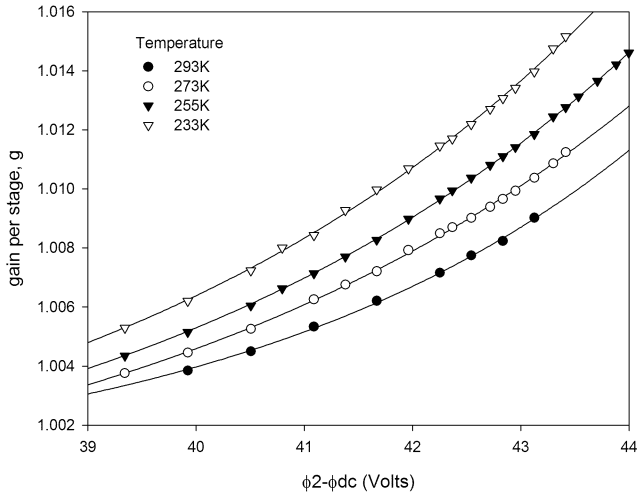

Fig. 4. Signal added per stage versus the difference between the peak potential of $\phi 2$ and the ϕdc level. Effect of temperature on the gain is also shown.

The total variance on the camera output signal is given by

$$\sigma_{\text{tot}}^2 = A^2 M^2 F^2 (\sigma_{\text{signal}}^2 + \sigma_{\text{dark}}^2) + A^2 \sigma_{\text{readout}}^2 \qquad (2)$$

where σ_{readout} is the readout noise, A is the video chain gain, σ_{signal} is the noise on the optically generated signal, S, σ_{dark} is the noise on the dark signal, S_{dark}

$$\sigma_{\text{signal}}^2 = S \quad \text{and} \quad \sigma_{\text{dark}}^2 = S_{\text{dark}}.$$

Therefore, the noise referenced to the image area σ_{eff} is simply given by

$$\sigma_{\text{eff}} = \sqrt{\left(F^2 (S + S_{\text{dark}}) + \frac{\sigma_{\text{readout}}^2}{M^2} \right)}.$$

It can be seen that setting the multiplication gain to a sufficiently high value virtually eliminates the effect of the readout noise. The multiplication gain is independent of readout rate and provides significant sensitivity enhancement even at high-frame rates. For example, subelectron noise can be readily achieved from a 128 × 128 pixel EMCCD operating at 1000 frames/s through a single output.

The amplitude of $\phi 2$ controls the field applied to the signal electrons and thus the probability of impact ionization and total gain. Typical curves for the gain per stage versus clock level are shown in Fig. 4. The fact that the $\phi 2$ amplitude controls the gain is very useful. A simple automatic gain control scheme

can be implemented where the output signal level controls the $\phi 2$ amplitude and/or an auto-iris within the camera lens. This technique provides operation over an extremely wide interscene dynamic range. For surveillance-type applications such cameras can cover light levels ranging from bright daylight to overcast starlight.

III. Noise Introduced by the Multiplication Process

A. Analytical Approach

A simple method for obtaining an analytical expression for the excess noise factor is shown here. First, consider a single multiplication stage.

Let n and m be the mean number of electrons into and out of the stage, respectively, σ_n^2 and σ_m^2 be the variance in the number of electrons into and out of the stage, g and σ_g^2 be the mean gain and variance in the gain

$$m = gn. \tag{3}$$

Assuming g is independent of n, then [11]

$$\frac{\sigma_m^2}{m^2} = \frac{\sigma_n^2}{n^2} + \frac{\sigma_g^2}{g^2}. \tag{4}$$

If the gain is treated as a Bernoulli process (i.e., the probability of multiplication is constant, and the outcomes of successive trials are independent), the number of electrons gained by the multiplication events can be described by the Binomial distribution. Therefore, the variance in the number of electrons added σ_{added}^2 is given by

$$\sigma_{\text{added}}^2 = n\alpha(1-\alpha)$$

where α is the probability of a multiplication event $= g - 1$ for small α

$$\sigma_g^2 = \frac{\sigma_{\text{added}}^2}{n^2} = \frac{\alpha(1-\alpha)}{n}. \tag{5}$$

Substituting (3) and (5) into (4) gives

$$\sigma_m^2 = (1+\alpha)^2\sigma_n^2 + n\alpha(1-\alpha). \tag{6}$$

Now, the N identical elements of the multiplication register can be considered. Let S_{in} and S_{out} be the mean input and output signals, respectively. Assuming the input signal is shot noise limited, its variance is simply S_{in}. The output variance σ_{out}^2 can be obtained by applying (6) to each stage in turn

For

$$N=1 \quad \sigma_{\text{out}}^2 = S_{\text{in}}(3\alpha+1)$$
$$N=2 \quad \sigma_{\text{out}}^2 = S_{\text{in}}(\alpha+1)(2\alpha^2+5\alpha+1)$$
$$N=3 \quad \sigma_{\text{out}}^2 = S_{\text{in}}(\alpha+1)^2(2\alpha^3+6\alpha^2+7\alpha+1).$$

For an arbitrary N

$$\sigma_{\text{out}}^2 = S_{\text{in}}(\alpha+1)^{(N-1)}\left(2(\alpha+1)^N + \alpha - 1\right)$$
$$= S_{\text{in}}M\left(\frac{2M+\alpha-1}{\alpha+1}\right). \tag{7}$$

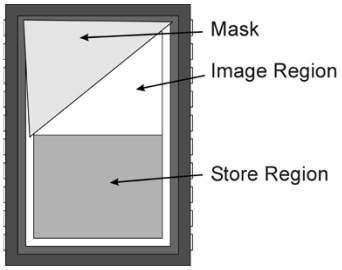

Fig. 5. Arrangement of the mask for the noise factor measurement.

Therefore, noting that $\sigma_{\text{in}}^2 = S_{\text{in}}$ and combining (7) and (1), we have

$$F^2 = \frac{1}{M}\left(\frac{2M+\alpha-1}{\alpha+1}\right) = 2(M-1)M^{-((N+1)/N)} + \frac{1}{M}. \tag{8}$$

This result is essentially the same as that obtained by Matsuo *et al*. [6] who considered the noise properties of a staircase avalanche photodiode. It is also equivalent to the results obtained for the staircase avalanche photodiode presented by Hollenhorst [7] who presented a rigorous mathematical approach to the calculation of noise for a wide range of cascaded multiplication devices. In this case, it is clear that when N and M are large F^2 tends to 2.

B. Experimental Measurement

1) Method: There are several direct methods that could be employed to measure the excess noise factor. For example, flat field images could be obtained and the noise in those images calculated. Alternatively repeated measurements could be made on a single pixel. Unfortunately, these methods introduce difficulties that can significantly affect the measurement. For example, illumination spatial nonuniformities or temporal fluctuations would dominate the measured distributions and lead to erroneous measurements. Therefore, a more robust method has had to be developed.

The device used for this study was a 512 × 512 pixel frame transfer device with 16 μm square pixels. The gain register has 536 multiplication elements. The method required that the device be run in continuous clocking mode, akin to that used in scanning time delay and integrate (TDI) applications. The CCD was masked diagonally as in Fig. 5 and illuminated. Lines were then continuously read out of the device. Once the output had settled, 1600 complete lines were stored. These lines formed the images to be analyzed. The mean signal and its variance along each column were calculated. Using the mask arrangement of Fig. 5 the mean signal increased approximately linearly in the direction perpendicular to the columns. Thus, a single image could provide the mean and variance values for a wide range of signal levels for a given multiplication gain. The maximum output signal was limited to 100 000 electrons to ensure that the signal level was low enough so that the output circuit and multiplication register linearity was better than 1%.

The mean output signal is given by

$$S_{\text{out}} = AM(S + S_{\text{dark}}) = AM(\sigma_{\text{signal}}^2 + \sigma_{\text{dark}}^2). \tag{9}$$

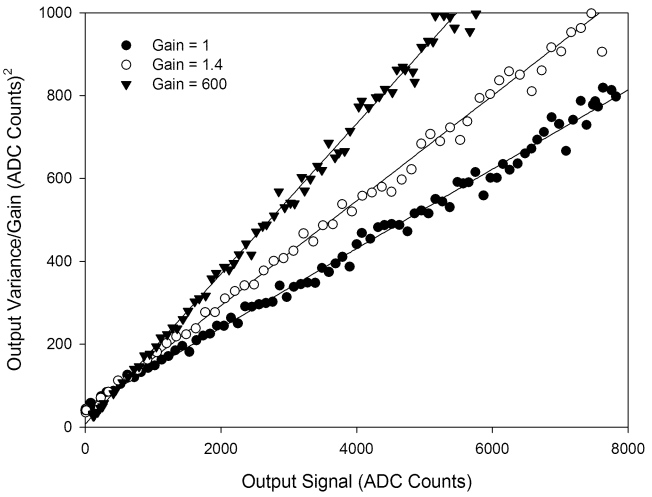

Fig. 6. Output variance divided by multiplication gain versus output signal for a range of multiplication gains. Temperature = 223 K. Only output from one column in every six is plotted for clarity.

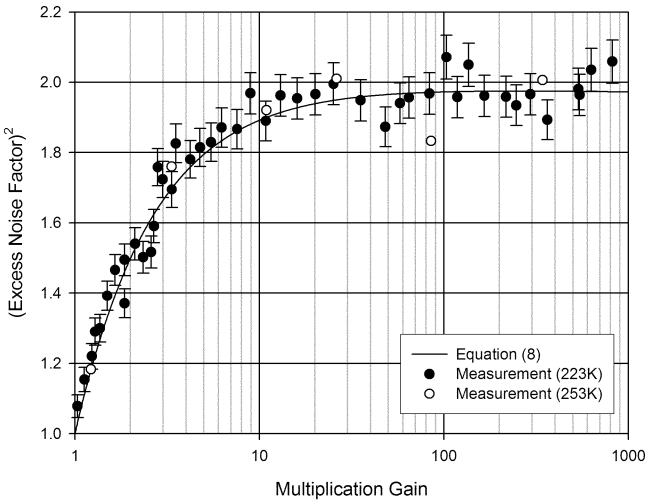

Fig. 7. Excess noise factor squared as a function of multiplication gain for a device having 536 multiplication elements.

Substituting (9) into (2) gives

$$\sigma_{\text{tot}}^2 = AMF^2 S_{\text{out}} + A^2\sigma_{\text{readout}}^2. \tag{10}$$

Therefore, with knowledge of the total video chain gain A and the multiplication gain M, the excess noise factor can be extracted from the gradient of a plot of σ_{tot}^2 versus S_{out}. The video chain gain was obtained using continuous scan images with the multiplication gain set to unity. In this case, the device operates as if it was a conventional CCD and the gradient of the mean variance plot gives the total video chain gain including the on-chip charge to voltage conversion factor. The multiplication gain was measured prior to acquiring each continuous scan image. For these measurements, the device was run in frame transfer mode and illuminated with a flat field. By measuring the mean signal with and without multiplication gain, the gain could be calculated. The integration time was extended when using no gain in order to obtain signals high enough to be measured reliably. It is estimated that using this method the uncertainty in the measurement of the multiplication gain was better than 3%. This dominates the uncertainty in the excess noise factor measurement as the error in the calculation of A was estimated to be better than 1%.

2) Results: Typical curves for the output variance divided by the multiplication gain versus output signal are shown in Fig. 6. Presented here are the curves for unity multiplication gain, a multiplication gain of 1.4 and 600. The gradient of a linear fit to the 600 gain data is approximately two times that of the fit to the unity gain data. This implies that the noise factor squared is around two, not unity as predicted in [4]. The measurement of the noise factor for a range of multiplication gains is presented in Fig. 7. Most of the measurements were made at a temperature of 223 K to eliminate dark signal, although some points were taken at a temperature of 253 K to test any temperature dependence. These points are also shown in the plot together with the theoretical prediction of (8).

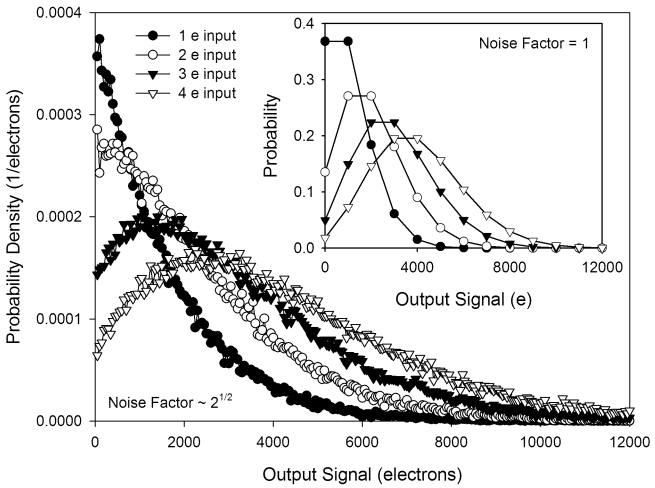

Fig. 8. Simulated output signal distribution for a range of mean input signal levels (zero dark signal). Input follows a Poisson distribution. The signal passes through 536 multiplication stages providing a total mean gain of 1000×. Inset shows the probability versus output assuming a noise factor of unity.

C. Monte Carlo Simulation

A Monte Carlo approach has been taken to simulate the output signal from an EMCCD. Both the optically generated signal and the dark signal are distributed according to Poisson statistics and the signal added by each stage of the multiplication register is assumed to follow a binomial distribution as in the derivation of (8). The process is repeated many times to obtain the output distributions of Fig. 8. The Monte Carlo sampling techniques for the required distributions are given in [12].

Fig. 8 shows the simulated output signal distribution from a device with 536 multiplication elements running with a multiplication gain of 1000. The inset is the output signal distribution obtained using a noiseless multiplication process. In this case, probability is plotted on the ordinate axis rather than probability density since the output is an integer multiple of 1000 and follows the Poisson distribution of the input. In both cases, photon

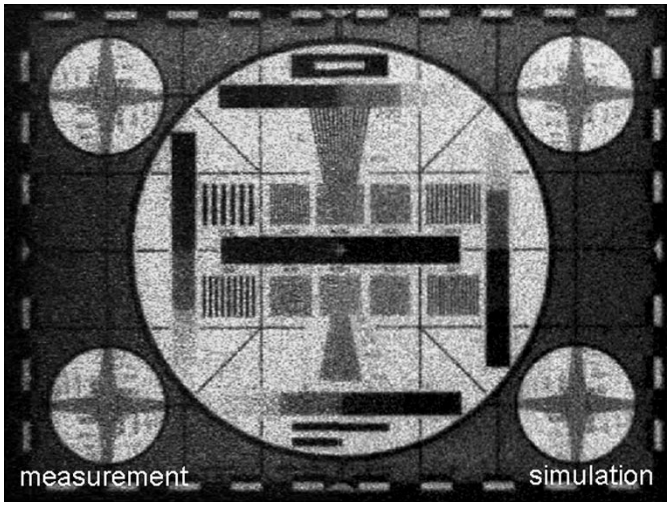

(a)

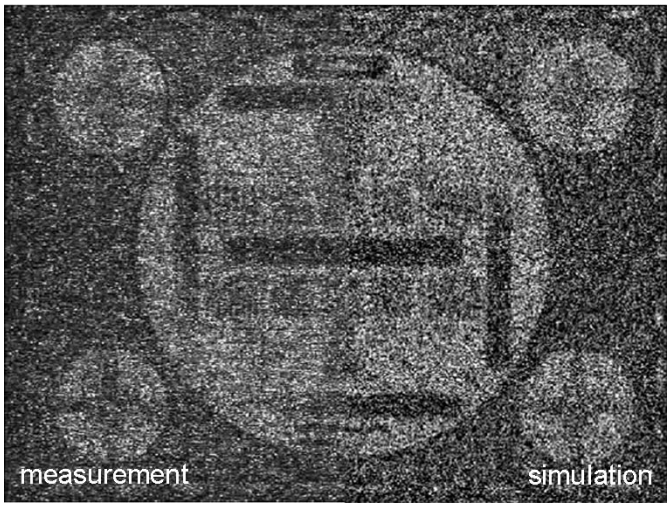

(b)

Fig. 9. Measured and simulated frames from the 625 line, 1-in format TV device running at 25 frames/s. Mean dark signal is 1.2 electrons/pixel. (a) "Starlight" mean signal = 10.4 electrons/pixel. (b) "Overcast Starlight" mean signal = 0.8 electrons/pixel. Left half of the image is the real frame, and the right half is taken from the simulated frame.

counting is clearly possible provided the counting threshold is above the readout and video chain noise. The fact that the multiplication process has a noise factor of $2^{1/2}$ has no effect on the single photon counting efficiency. The sensor's photon counting capability will be the subject of a future paper.

This simulation technique can be usefully extended to simulating the imaging performance by using the mean value of each pixel in a frame as the input. Many output frames can be generated this way and combined to form a realistic simulation of the output video. Typical results are shown in Fig. 9. These images were taken with a 1-in format TV device running at CCIR video frame rates (25 frames/s) at -3 °C. This device has a pixel size of 20 μm $\times$ 30 μm for the 625 line variant and 591 multiplication elements. The mean signal levels for the frame were measured by monitoring the reset drain current. The signal modulation was calculated using a chart image taken at high-light level and unity multiplication gain. The pixel values of this image were scaled according to the required mean signal level and then used as the input to the Monte Carlo procedure which generates the photon shot noise and multiplication noise. The signal levels chosen for this demonstration approximately correspond to those obtained from scenes illuminated with starlight ($\sim$0.001 lx) and overcast starlight ($\sim$0.0001 lx) through an $f/1.4$ lens. The results of the simulations are shown alongside the measurements. As these are still frames they do not benefit from the temporal integration of the eye, which tends to reduce the noise and increase the perceived resolution. Even so, they show that very useful performance can be obtained even at extremely low-light levels.

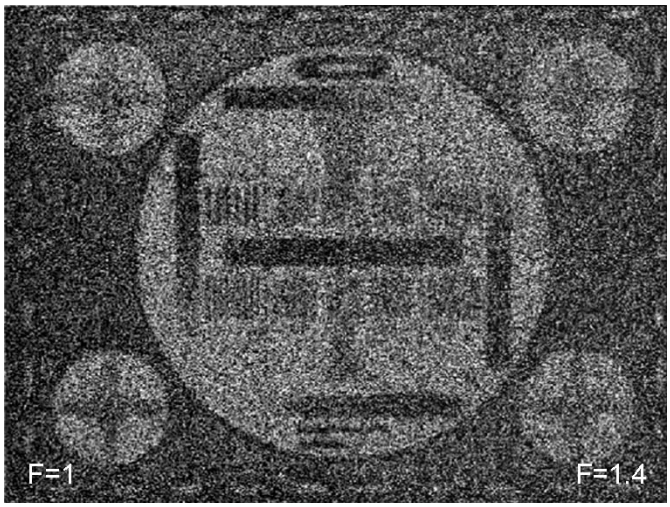

Fig. 10. Simulation under conditions of Fig. 9(b) showing the effect of the multiplication register. Simulation on the left-hand side of the image includes only photo electron and dark signal shot noise (zero readout/video chain noise). Right-hand side includes the effect of the multiplication register.

The effect that multiplication noise has on the subjective imaging performance can be established by running the Monte Carlo simulation with and without the gain register and assuming zero readout and video chain noise. The results are shown in Fig. 10. Although there is some difference in the image quality the impact of the multiplication noise is small.

IV. Conclusion

A robust method for measuring the excess noise factor has been developed and the results show that the multiplication register of an electron multiplying CCD behaves like an ideal staircase avalanche photodiode; for a multiplication gain greater than about 10 times the noise factor reaches its maximum value of about 1.4. The theoretical approach has only considered the noise due to the discrete nature of the multiplication process. The noise due to the fluctuation in the gain mechanism itself has not been considered. However, the excellent agreement between the experiment and theory indicates that the impact this has on the noise factor for the devices tested here is minimal.

The agreement between the simulated and the actual video performance of the EMCCD sensors is excellent, showing that the devices tested operate very close to the theoretical optimum performance for an imaging sensor. The fact that the noise factor is $\sim$1.4 rather than unity has little effect on the subjective image quality, even at the very lowest light levels. However, this may depend on the subject and circumstances of the observation.

REFERENCES

[1] S. K. Madan, B. Bhaumik, and J. M. Vasi, "Experimental observation of avalanche multiplication in charge coupled devices," *IEEE Trans. Electron Devices*, vol. ED-30, pp. 694–699, June 1983.

[2] P. Jerram *et al*., "The LLLCCD: Low light imaging without the need for an intensifier," *Proc. SPIE*, vol. 4306, pp. 178–186, 2001.

[3] R. N. Tubbs, J. E. Baldwin, C. D. Mackay, and G. C. Cox, "Diffraction-limited CCD imaging with faint reference stars," *Astronomy Astrophys*., vol. 387, pp. L21–L24, 2002.

[4] J. Hynecek, "Impactron—A new solid state image intensifier," *IEEE Trans. Electron Devices*, vol. 48, pp. 2238–2241, Oct. 2001.

[5] S. E. Moran, B. L. Ulich, W. P. Elkins, R. L. Strittmatter, and M. J. Deweert, "Intensified CCD (ICCD) dynamic range and noise performance," *Proc. SPIE*, vol. 3173, pp. 430–457, 1997.

[6] K. Matsuo, M. C. Teich, and B. E. A. Saleh, "Noise properties and time response of the staircase avalanche photodiode," *IEEE Trans. Electron Devices*, vol. ED-32, pp. 2615–2623, 1985.

[7] J. N. Hollenhorst, "A theory of multiplication noise," *IEEE Trans. Electron Devices*, vol. 37, pp. 781–788, Mar. 1990.

[8] J. Hynecek and T. Nishiwaki, "Recent progress toward single photon detection using charge multiplying CCD image sensors," in *Proc. 16th World Multiconf. Syst. Cybern*., July 2002, no. 2, pp. 7–12.

[9] C. D. Mackay, R. N. Tubbs, R. Bell, D. J. Burt, P. Jerram, and I. Moody, "Sub-electron read noise at MHz pixel rates," *Proc. SPIE*, vol. 4306, pp. 289–298, 2001.

[10] D. J. Burt and R. T. Bell, "CCD Imager," GB patent 2 323 471, Mar. 22, 1997, granted Apr. 17, 2002.

[11] M. L. Boas, *Mathematical Methods in the Physical Sciences*, 2nd ed. New York: Wiley, p. 734.

[12] K. Hagiwara *et al*., "Reviews, tables, and plots in the 2002 review of particle physics," *Phys. Rev. D*, vol. 66, 010 001, 2002.

Mark Stanford Robbins (M'00–SM'02) was born in the U.K. in 1966. He received the B.Sc. (Hons) degree in applied physics in 1989 and the Ph.D. degree in radiation damage of CCDs in 1992, both from Brunel University, Oxbridge, U.K.

In 1992, he was appointed Research Fellow working with the CERN RD20 collaboration on the theoretical modeling of the radiation damage effects in silicon strip detectors for the LHC. Since 1994, he has been with EEV Ltd. (now known as E2V Technologies, Chelmsford, U.K.) working on the development and application of technologies for x-ray and optical imaging. He is a Technical Manager for the L3Vision sensor program. He has authored and coauthored several papers in the field of radiation damage effects and imaging.

Dr. Robbins is a member of the Institute of Physics and is a Chartered Physicist. He has participated in the paper review process for the IEEE TRANSACTIONS ON NUCLEAR SCIENCE and various international conferences.

Benjamin James Hadwen was born in the U.K. in 1976. He received the M.Phys. degree in physics from Oxford University, Oxford, U.K., in 1999.

Since 1999, he has been working for E2V Technologies, Chelmsford, U.K., on the development and characterization of advanced imaging technologies. He is currently a member of the L3Vision sensor development group.